Intrinsic Impurities in Glass Alkali-Vapor Cells

B. Patton, K. Ishikawa,* Y.-Y. Jau, and W. Happer

Joseph Henry Laboratory, Department of Physics, Princeton University, Princeton, New Jersey 08544, USA

(Received 30 January 2007; published 11 July 2007)

We report NMR measurements of metallic ^{133}Cs in glass cells. The solid-liquid phase transition was studied by observing the NMR peaks arising from these two phases; surprisingly, many cells yielded two additional NMR peaks below the melting point. We attribute these signals to two distinct impurities which can dissolve in the liquid alkali metal and affect its chemical shift. Intentional contamination of cesium cells with O_2 confirms this hypothesis for one peak. The other contaminant remains unknown but can appear in evacuated cells. Similar effects have been seen in ^{87}Rb cells.

DOI: 10.1103/PhysRevLett.99.027601 PACS numbers: 76.60.Cq, 32.30.Dx, 64.75.+g

Glass alkali-vapor cells have found widespread use in research, being crucial for spin-exchange optical pumping [1], atomic magnetometry [2,3], and precision frequency standards [4]. Typically these cells are loaded with alkali metal under high vacuum before being filled with any buffer gases and then permanently sealed. Despite the simplicity of this procedure, considerable variation in performance (e.g., noble-gas relaxation times or alkali-metal vapor densities) is often seen from one cell to the next. In this Letter, we present ^{133}Cs nuclear magnetic resonance (NMR) data which demonstrate that the alkali metal is often contaminated during cell fabrication. We conclusively identify one contaminant as oxygen and show that another unknown impurity can result solely from glass–alkali-metal interactions.

It is well-known [5] that newly-manufactured spin-exchange optical pumping cells exhibit noble-gas nuclear relaxation times which gradually stabilize to their equilibrium values over several days. Similarly, atomic clock cells often experience a slow change in alkali-metal vapor density over many months, even after initial equilibration of the vapor signal [6]. Such changes in alkali-metal density can cause systematic shifts in the time base and ultimately limit clock precision [7].

This curing process can be attributed to interactions between the alkali metal and the cell walls. NMR can be used to analyze these interactions—this is demonstrated in Fig. 1, which shows ^{133}Cs NMR data taken as a vapor cell was warmed above the cesium melting temperature $T_m = 28.52\,^{\circ}$C and then cooled. The measured NMR frequency is plotted vs temperature, with an example spectrum included (inset). Below T_m, the NMR peak of solid cesium can be seen. This signal disappears upon melting and is replaced by the lower-frequency NMR signal of the liquid. Both the solid and the liquid show a decrease in Larmor frequency with increasing temperature; this is due to thermal expansion of the metal and agrees well with prior data [8].

Other features of this graph are quite surprising. The liquid NMR signal does not vanish when the cell is cooled below T_m. This phenomenon is observed no matter how slowly the temperature of the cell is decreased, so it is not due to delayed thermal equilibration of the sample. Most intriguing, this graph reveals the existence of a third peak (labeled [α]) whose frequency *increases* with increasing temperature, merging with the liquid signal at T_m. This peak is clearly visible in the raw spectrum. It is this unusual NMR signal which constitutes the focus of the present Letter.

Alkali-metal NMR frequencies can be sensitive to chemical impurities through changes in the Knight shift, a frequency shift which arises from conduction-band electrons in the metal [9]. Each nucleus sees on average one free electron with which it is coupled through the hyperfine interaction $A\mathbf{I}\cdot\mathbf{S}$. The conduction-band electrons are partially polarized by the external magnetic field; this results in an upward shift of the metal's NMR frequency (on the order of a percent) with respect to that of the same nucleus in a nonmetallic compound (e.g., CsCl). The Knight shift is typically reported [10] as the dimensionless number

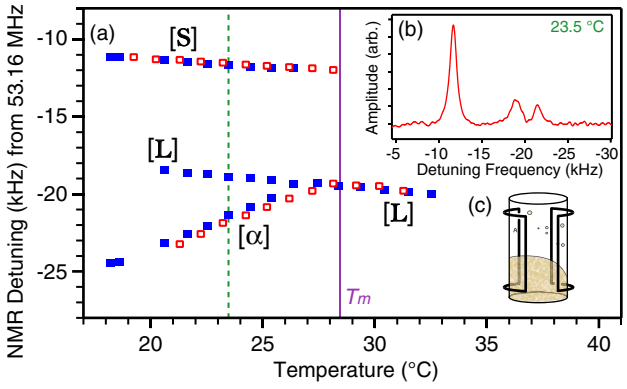

FIG. 1 (color online). (a) ^{133}Cs NMR frequency plotted as the cell temperature is increased (open squares) past the melting point T_m and then decreased (filled squares). (b) Sample Fourier transform spectrum taken at 23.5 °C (dashed line). Three NMR peaks are clearly visible. (c) Schematic of the cell and NMR coil. For these data, the cell was a 1/2-inch diameter Pyrex cylinder filled with Cs and 400 Torr N_2.

$$K = (\nu_m - \nu_r)/\nu_r, \quad (1)$$

where ν_m is the metallic NMR frequency, and ν_r is the frequency of the nonmetallic reference compound. Any trace impurity dissolved in the alkali metal can affect K by changing the density of free electrons.

For this experiment, cells made of either Pyrex or GE 214 (fused silica) were sealed to a Pyrex string attached to a vacuum manifold. Either a Pyrex retort filled with cesium chloride and calcium chips or a breakseal ampoule of cesium (UMC Corp., Chemetall GmbH) was attached to the string. An oven was placed around the cells and set to 350 °C while the manifold was evacuated with a turbopump. The cells were baked at this temperature for several days until the residual pressure fell below $\sim 5 \times 10^{-8}$ Torr (measured by a cold cathode gauge near the pump); then, the oven was turned off. The cesium was moved into the string either by heating the retort with a flame (thus liberating Cs vapor through the reaction $2CsCl + Ca \rightarrow 2Cs + CaCl_2$) or by breaking the seal on the cesium ampoule with a glass-coated magnetic hammer. The cesium was then loaded into each cell by heating the string with a low flame, which moved the alkali metal through the string by a combination of fluid flow and condensation. Once all the cells had been filled with a Cs film, the manifold was filled with any buffer gases, and the stem of each cell was softened with a torch and pulled off to make a permanent seal. The buffer gases flowed through a chemical getter (NuPure Corp.) to remove impurities. The above procedure was designed to minimize chemical contamination and is the standard method used to make high-purity alkali-vapor cells. ^{87}Rb cells were filled in an identical fashion, with enriched ^{87}RbCl and calcium chips providing the rubidium.

NMR was performed in a 9.4 T (53.15 MHz ^{133}Cs, 131.5 MHz ^{87}Rb) superconducting magnet (Oxford Instruments) on a custom-made spectrometer. Because of the short longitudinal relaxation times T_1 of alkali metals (< 1 ms for both ^{87}Rb and ^{133}Cs), free induction decays (FIDs) could be averaged on a Yokogawa DL708E oscilloscope at a rate of 4000/ min. Extensive averaging was necessary because the RF skin depth in cesium is roughly 30 μm at this frequency, so only a small fraction of the Cs was excited by the NMR pulse. Generally, 4000 to 40 000 traces were averaged for each FID, which was then Fourier transformed on a PC and fit to one or more Lorentzians. The center frequency of each Lorentzian fit was used as that peak's NMR frequency. Temperature data were taken by a resistive thermal device (RTD) placed near the cell and were recorded concurrently with the FIDs. The probe was heated with a counter-wrapped resistive wire which produced a magnetic field of less than 0.05 ppm at the NMR coil. Sufficient time was allowed between temperature points to ensure thermal equilibration of the cell. We also performed NMR measurements on sealed Cs ampoules before using them to fill cells.

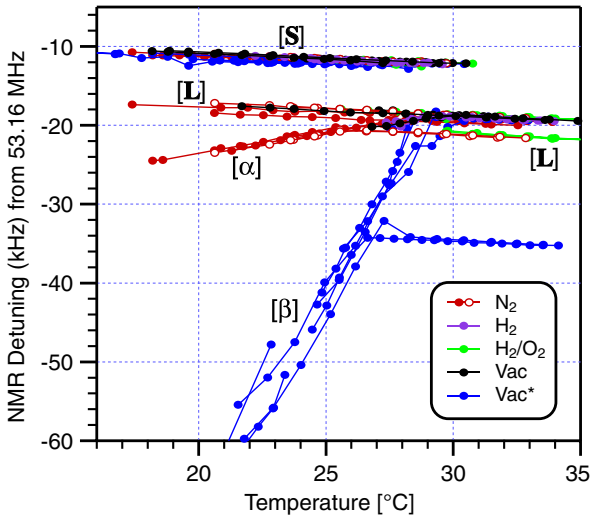

FIG. 2 (color online). NMR data from many Cs cells. Color indicates the type of buffer gas (legend). Cells include those filled with N_2 gas, H_2 gas, H_2/O_2 mixtures, evacuated cells suspected of contamination (Vac*), and vacuum cells with no sign of impurities (Vac). Filled data points are Pyrex cells; open data points are GE 214 cells.

Figure 2 contains thermal cycle data from many cesium cells. The most striking feature of this plot is that there are *two* distinct peaks which may occur in the ^{133}Cs NMR spectrum in addition to the solid and liquid signals. We shall refer to the peak with the shallower (steeper) slope as the α (β) peak. These two signals seem to be mutually exclusive, as no cell has yielded both; moreover, neither peak's presence correlates with the method used to fill the cells with cesium (i.e., CsCl or Cs ampoule). The two cells which exhibited strong β peaks also had the strongest evidence of chemical contamination—one was a decades-old cesium ampoule (UMC Corp.), and the other was an evacuated cell whose cesium remained liquid at room temperature. Based upon this observation, we hypothesize that the additional NMR signals are caused by chemical impurities which dissolve in the liquid alkali metal and reduce the free electron density and thus the ^{133}Cs Knight shift.

If a sample of liquid cesium is exposed to a soluble impurity X at a concentration $[X]$, the cesium will become uniformly contaminated and produce a single NMR peak (Fig. 3). The chemical shift of this peak will depend on $[X]$ and will tend toward lower frequencies if X is electronegative, since the cesium atoms will act more like Cs^+ ions. Upon cooling, the impure liquid cesium will exhibit depression of its freezing point; below this temperature, nearly-pure solid cesium will begin to crystallize out of the solution and a solid NMR peak will appear. As the cell is cooled further, cesium atoms will be transferred from the liquid phase to the solid, increasing $[X]$ in the remaining Cs-X solution. The effect on the NMR spectrum will be twofold: the amplitude of the remaining liquid peak will

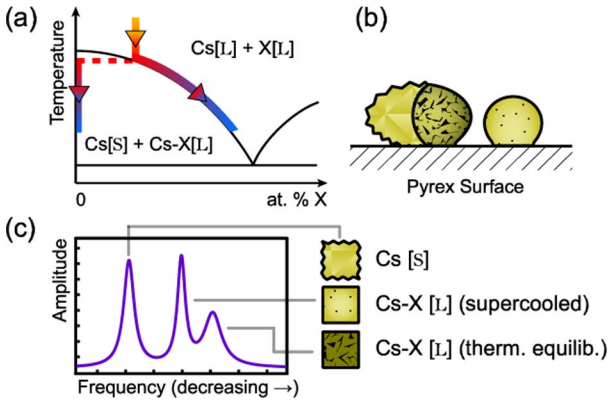

FIG. 3 (color online). Proposed freezing mechanism for contaminated liquid Cs. (a) A typical binary phase diagram for Cs and an impurity X. (b) Some droplets reach thermal equilibrium (left), whereas some exhibit supercooling (right). (c) Simulated NMR spectrum which reflects this scenario.

drop as cesium atoms condense into the solid phase, and its frequency will rapidly decrease as the mixture approaches a compoundlike ratio of Cs and X. Though this hypothesis only predicts two NMR signals, the observed spectra can be explained if some of the alkali metal undergoes supercooling down to room temperature. This is plausible given that the cesium "film" actually consists of a spray of small, randomly-sized droplets; and it is known that the degree of supercooling depends acutely on particle size [11]. Additional evidence of supercooling is that cells with a single large drop of cesium never demonstrate a liquid peak below T_m.

It is possible to test this hypothesis with oxygen as impurity X since the binary phase diagram has been measured for the Cs-O system [12]. Cesium can form several stable suboxides, starting with Cs_7O. At lower oxygen fraction [O], the melting point of the metallic Cs-O mixture decreases in a nearly linear fashion from 28.52 °C (pure cesium) to −0.36 °C at the eutectic point ([O] = 0.09). Cells with accidental oxygen contamination will likely occupy this region of the phase diagram. As a Cs-O sample is cooled, a vertical path of decreasing temperature on the phase diagram intersects the coexistence curve at the depressed freezing point and then follows the curve as illustrated in Fig. 3. At any temperature below the freezing point, the ratio of pure solid to contaminated liquid cesium will be uniquely determined by the phase diagram. This in turn fixes the oxygen percentage in the liquid and thus the ^{133}Cs Knight shift of the β peak. Thus all cells, regardless of their oxygen content, will exhibit the same frequency vs temperature curve for their β peaks. Cells with different values of [O], however, will have different frequency shifts in the homogeneous liquid above T_m and will display different degrees of freezing point depression. By examining the temperature dependence of the β peak frequency and comparing it to the Cs-O phase diagram, it should be possible to determine K as a function of [O]. Then, we can determine [O] for a given cell by measuring the NMR frequency shift of the homogeneous liquid above T_m.

For this experiment, we created cells which had small amounts of oxygen as a contaminant. The procedure of making the cells was the same as before, except O_2 gas was allowed to flow into the vacuum system at pressures of $\sim 10^{-6}$ Torr during the cesium filling process. The pressure (as measured by the cold cathode gauge near the turbopump) fluctuated as O_2 was absorbed by the cesium, making it difficult to quantify the Cs-O ratio by pressure data alone. Nonetheless, since the cells were pulled off sequentially, they represent a range of oxygen contaminations. Indeed, the last two cells to be sealed contain Cs which remains liquid at room temperature.

Figure 4 shows data taken from thermal cycles of two such cells, along with the earlier β peak cells. A small temperature shift was applied to each group to account for changes in the RTD position. The size of this offset was determined by taking concurrent NMR spectra of very pure Cs samples (not shown in Fig. 4) and setting their melting point to 28.52 °C in accordance with Ref. [12]. The slopes of the β peaks match up exactly, and their amplitudes correlate with the amount of O_2 in the intentionally contaminated cells, proving that oxygen is responsible for the β peak. From the pure Cs ampoules, the Knight shift of liquid Cs at T_m was measured to be 1.4759% with respect to a dilute aqueous solution of CsCl at room temperature. This is in excellent agreement with prior data [10]. Because the β peak's temperature dependence should be the same for all cells, all of the β peak data points were grouped together to calculate the dependence of the Knight shift on [O]. The temperature of each data point was compared to the Cs-O phase diagram to extract a value

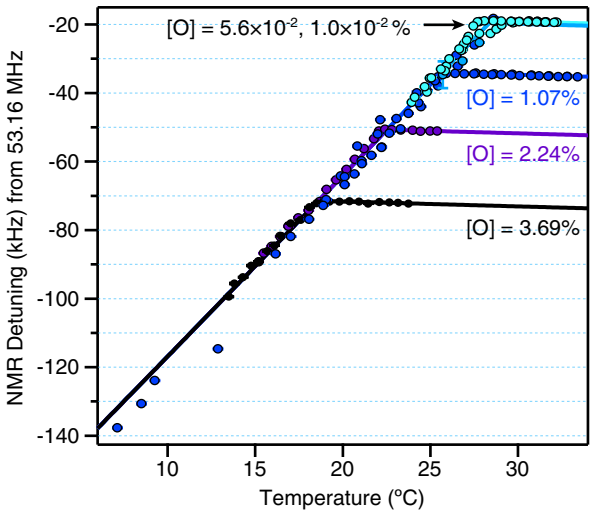

FIG. 4 (color online). Data from five cells which exhibited the β peak. The two lowest curves correspond to cells which were intentionally contaminated with O_2. Solid lines show the prediction of Eq. (2) assuming the best-fit oxygen concentration for each cell.

for [O] at that temperature, and then the oxygen dependence of K was varied to optimize the fit to the β peak data set. This gave

$$K = 1.4759(4) \times 10^{-2} - 2.80(2) \times 10^{-2} \cdot [\mathrm{O}] - 2.70(2) \times 10^{-6} \cdot (T - 28.52\,^{\circ}\mathrm{C}). \quad (2)$$

The temperature dependence of K was measured independently. Equation (2) is valid both above and below the freezing point—above it, [O] is constant for a given cell; but below it, [O] is related to the temperature through the binary phase diagram. Finally, we extracted [O] for each cell by fitting its liquid peak frequency shift to Eq. (2) above the melting point. Figure 4 includes the predicted NMR frequency for each cell (solid lines) calculated by inserting this best-fit oxygen percentage into Eq. (2)—the agreement with experiment is excellent.

Our measurement of the Knight shift yields a stronger dependence on [O] (roughly 20% larger) than previously reported in the literature [13]. Nonetheless, our value is plausible in view of a very simple model of the Knight shift. For a fixed total number of atoms in a Cs-O mixture, the number of oxygen atoms will scale as the atomic percentage [O] and the number of cesium atoms as $(1 - [\mathrm{O}])$. Assuming that each Cs atom contributes one electron to the mixture and each oxygen atom removes two electrons, the number of free electrons in the metallic Cs will scale as $(1 - 3[\mathrm{O}])$. The Knight shift is proportional to the number of free electrons per Cs atom:

$$K = K_0 \frac{1 - 3[\mathrm{O}]}{1 - [\mathrm{O}]} \underset{[\mathrm{O}] \ll 1}{\longrightarrow} K_0(1 - 2[\mathrm{O}]), \quad (3)$$

where K_0 represents the Knight shift for pure cesium. With this semiquantitative picture of homogeneous electron depletion, we would predict that the oxygen-dependent term in Eq. (2) should be twice as large as the pure Cs Knight shift—quite nearly what we measured. The discrepancy with Ref. [13] could be due to the experimental technique—in previous works a different cell was made for each oxygen concentration studied, increasing the chances of error in oxygen measurement or the possibility of inhomogeneous mixtures of oxygen-rich stable suboxides and cesium-rich liquid [14]. Our data have the advantage that a range of [O] can be explored with a single cell simply by lowering the temperature below the nominal freezing point.

The α peak exhibits the same characteristics as the β peak except with a shallower slope. This leads us to conclude that it too is the result of an impurity, though one with a lower electronegativity or Cs solubility than oxygen. Significantly, this peak is evident even in evacuated cells which were prepared very carefully so as to eliminate all impurities—this leads us to conclude that its only possible source is the glass used for the cells. So far we have been unable to reproduce the α peak by intentional contamination of cells with elemental silicon, SiO_2 powder, or H_2 or N_2 gas. An analogous peak has also been observed in ^{87}Rb cells filled with N_2 gas and made from different glasses.

If the α and β peaks are due to an intrinsic and ongoing reaction between the alkali metal and the cell walls, these contaminants could pose a serious problem for hot vapor atomic clocks since they could produce a frequency shift by reducing the alkali-metal-vapor density [7]. Further studies are warranted to determine the effect of these impurities on long-term equilibration in atomic frequency standards. On the other hand, the β peak may actually prove beneficial in spin-exchange optical pumping cells because of the decreased ^{3}He wall relaxation rates in cells coated with alkali-metal suboxides [15].

In conclusion, we have used ^{133}Cs NMR to detect two impurities in alkali-vapor cells and identify one of them as oxygen. The other impurity can arise in pristine glass cells, raising the concern that chemical reactions in these cells may introduce impurities throughout their lifetimes.

The authors would like to thank Mike Souza for his advice and glassblowing skills, as well as Chemetall GmbH for the high-purity Cs samples. This work was supported by the Air Force Office of Scientific Research.

*Present address: Graduate School of Material Science, University of Hyogo, Japan

[1] T. G. Walker and W. Happer, Rev. Mod. Phys. **69**, 629 (1997).
[2] H. Xia, A. B.-A. Baranga, D. Hoffman, and M. V. Romalis, Appl. Phys. Lett. **89**, 211104 (2006).
[3] I. K. Kominis, T. W. Kornack, J. C. Allred, and M. V. Romalis, Nature (London) **422**, 596 (2003).
[4] S. Knappe, V. Gerginov, P. D. D. Schwindt, V. Shah, H. G. Robinson, L. Hollberg, and J. Kitching, Opt. Lett. **30**, 2351 (2005).
[5] Z. Wu, W. Happer, M. Kitano, and J. Daniels, Phys. Rev. A **42**, 2774 (1990).
[6] S. Herbulock, C. Klimcak, A. Presser, J. Milne, and J. Camparo, in *Procedings of the 35th Annual PTTI Meeting* (2003), pp. 435–443.
[7] S. Micalizio, A. Godone, F. Levi, and J. Vanier, Phys. Rev. A **73**, 033414 (2006).
[8] B. R. McGarvey and H. S. Gutowsky, J. Chem. Phys. **21**, 2114 (1953).
[9] C. H. Townes and W. D. Knight, Phys. Rev. **77**, 852 (1950).
[10] W. W. Warren, G. F. Brennert, and U. El-Hanany, Phys. Rev. B **39**, 4038 (1989).
[11] D. Turnbull and R. E. Cech, J. Appl. Phys. **21**, 804 (1950).
[12] A. Simon, Z. Anorg. Allg. Chem. **395**, 301 (1973).
[13] Y. Tsuchiya, E. F. W. Seymour, and G. A. Styles, J. Phys. Condens. Matter **6**, 3889 (1994).
[14] G. Brauer, Z. Anorg. Allg. Chem. **255**, 101 (1947).
[15] A. Deninger, W. Heil, E. W. Otten, M. Wolf, R. K. Kremer, and A. Simon, Eur. Phys. J. D **38**, 439 (2006).